Relativity, Nuclear Polarizability, and Screening in Sub-Coulomb Elastic Scattering

W. G. Lynch,[a] M. B. Tsang,[a] H. C. Bhang,[b] J. G. Cramer, and R. J. Puigh[c]
Nuclear Physics Laboratory, University of Washington, Seattle, Washington 98195
(Received 29 October 1981)

Elastic scattering of p-shell nuclear projectiles from ^{208}Pb has been examined for deviations from Rutherford scattering. Four effects can be important: atomic screening, vacuum polarization, nuclear polarizability, and a relativistic effect of dynamical origin. The presence of atomic screening, nuclear polarizability, and the relativistic effect was observed, thus constituting the first measurement of this relativistic effect using complex nuclei and the first measurement of nuclear polarizability in an external Coulomb field.

PACS numbers: 25.70.Hi, 11.10.Qr, 21.10.Ky, 24.90.+d

Measurements of Coulomb excitation and Coulomb-nuclear interference have long relied on the dominance of the Coulomb force in sub-Coulomb nuclear scattering to determine nuclear deformations and other spectroscopic quantities. It has been known for some time that accurate measurement of these quantities can require correction for small effects such as nuclear polarizability, atomic screening, and relativistic effects.[1,2] In addition, exotic phenomena such as the formation of superheavy quasimolecules have been suggested to occur for colliding heavy nuclei.[3] Despite their relevance, these effects have eluded measurement because of their discouragingly small size in systems and energies where Coulomb excitation can be neglected. For p-shell nuclei scattering from ^{208}Pb where such isolation can be made, four effects are important at the 0.1% level.

(1) *Relativistic effect.*—One can isolate this nonkinematic relativistic correction to Rutherford scattering by examining the Klein-Gordon equation for a particle in a Coulomb potential $V_{\rm Coul}$:

$$(\vec{P}^2c^2+m^2c^4)\psi=(E-V_{\rm Coul})^2\psi$$
$$=(E^2-2EV_{\rm Coul}+V_{\rm Coul}^2)\psi, \qquad (1)$$

where E is the total energy of the particle (including the rest mass) and $\vec{P}^2=\hbar\nabla^2$. The Klein-Gordon equation given here differs in form from the corresponding Schrödinger equation principally by the additional term proportional to $V_{\rm Coul}^2$. This $V_{\rm Coul}^2$ term causes the fine-structure splitting in pionic atoms which has only been measured recently in pionic titanium.[4] For the heavy-ion systems discussed in this work, this term causes an observable deviation $\Delta=(\sigma-\sigma_{\rm Ruth})/\sigma_{\rm Ruth}$ from Rutherford scattering.

(2) *Nuclear polarizability.*—When the target and projectile are separated but in close proximity, both nuclei are excited virtually to the giant resonances, particularly the giant dipole resonance. Since the giant dipole resonance dominates the photoabsorption cross section one can express the effective potential $V_{\rm cex}$ for nuclear polarizability in terms of the inverse-energy–weighted photosum σ_{-2}[5,6]:

$$V_{\rm cex}=-0.5\frac{e^2hc}{2\pi^2r^4}(Z_1^2\sigma_{-2}^{(2)}+Z_2^2\sigma_{-2}^{(1)}), \qquad (2)$$

where $\sigma_{-2}^{(i)}=\int_0^\infty(dE/E^2)\sigma^{(i)}(E)$, $\sigma^{(i)}(E)$ is the photoabsorption cross section for nucleus i, and eZ_i is the charge of nucleus i. The values of σ_{-2} used in these calculations are 0.316,[7] 0.44,[8] 0.44, 0.585,[7] and 16.0 for ^{12}C, ^{14}N, ^{15}N, ^{16}O, and ^{208}Pb, respectively.

(3) *Electron-positron vacuum polarization.*—For point nuclei vacuum polarization is accurately described by the Uehling potential $V_{\rm Ueh}$[9]:

$$V_{\rm Ueh}=\frac{2Z_1Z_2\alpha e^2}{3\pi r}\int_1^\infty dt\exp\left(-\frac{2r}{\lambda\!\!\!^{-}_e}t\right)\left(\frac{1}{t^2}+\frac{1}{2t^4}\right)(t^2-1)^{1/2}, \qquad (3)$$

where α is the fine-structure constant and $\lambda\!\!\!^{-}_e$ is the reduced electron wavelength (386 fm). For finite nuclei, $V_{\rm Ueh}$ should be folded over the charge densities of the projectile and target nuclei thus obtaining $V_{\rm pol}$ which contains finite-size corrections to $V_{\rm Ueh}$.[10]

(4) *Electron screening.*—Calculations show that the effects of electron ionization of the K and L shells are negligible and that polarization of the K shell is very small at most energies, especially for $E_{\rm lab}\geq 20$ MeV. We therefore use a static

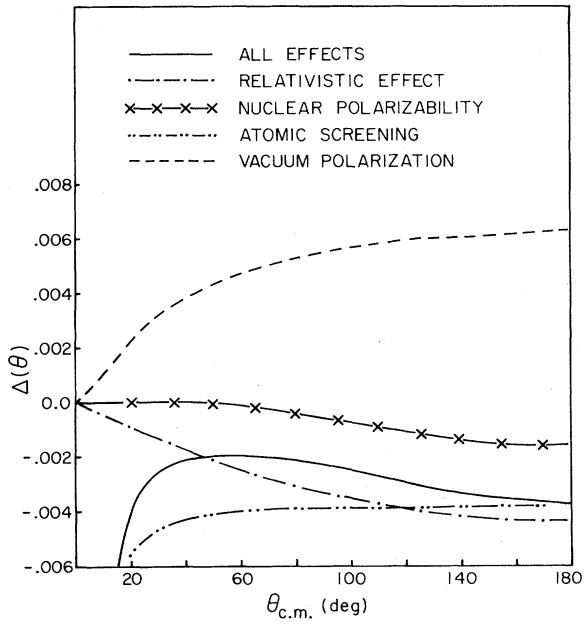

FIG. 1. Five theoretical predictions of Δ as a function of center-of-mass scattering angle for 50-MeV $^{16}O+^{208}Pb$.

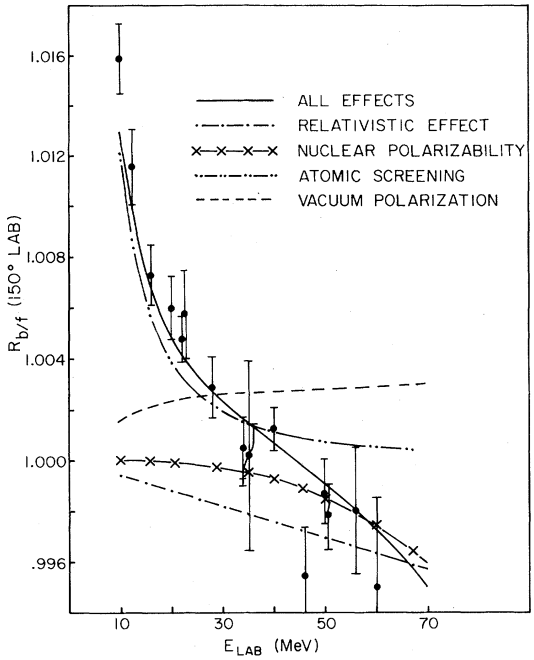

FIG. 2. Five theoretical predictions of $R_b/_f$(150°(lab)) for $^{16}O+^{208}Pb$ as a function of E_{lab}. Corresponding experimental measurements of $R_b/_f$ are also plotted.

screening potential V_{sc} derived from relativistic Hartree-Fock electron wave functions.[11]

The deviation Δ for each of these effects taken separately is plotted as indicated in Fig. 1. The theoretical curves were obtained by using the classical approximation of Newtonian mechanics. Excellent agreement (1 part in 10^5) was obtained when this calculation of the relativistic effect was compared to the quantum-mechanical solution of Eq. (1).[12] The solid line in Fig. 1 is the calculation of the total deviation from Rutherford scattering when all of the above effects are considered simultaneously. One can see that screening is the largest correction at forward angles while the other three effects become more important at large angles.

In this Letter we describe the measurement of sub-Coulomb elastic scattering with the systems (^{12}C, ^{14}N, ^{15}N, ^{16}O)$+^{208}Pb$. To measure these small effects (few tenths of 1%), the experiment was designed to constrain the total systematic error below 0.05%. This accuracy requirement precludes the measurement of angular distributions since such measurements require the determination of absolute scattering angles to essentially unattainable precision. Instead, we measured the energy dependence of the cross section ratios $\sigma(\theta_{lab})/\sigma(30°(lab))$ at fixed angles where $\theta_{lab}=140°$, 145°, 150°, 160°, and 170°. Since the angular dependence of the Rutherford cross section is energy independent, any energy dependence in these ratios is caused by one or more of the four effects mentioned earlier. In Fig. 2 we have plotted the ratio $R_{b/f}(150°(lab))=[\sigma(150°)/\sigma_{Ruth}(150°)]\sigma_{Ruth}(30°)/\sigma(30°)$, where $\sigma(\theta)$ is the cross section for elastic scattering when one or all of the above effects have been included. Since we are measuring the energy dependence of $R_{b/f}$, one can see that at energies below 20 MeV atomic screening is the dominant effect because of its effect on the forward-angle cross section. As the energy is increased the relativistic effect and nuclear polarizability become comparatively more important and dominate above 40 MeV.

The experimental data were taken in the 152-cm scattering chamber of the University of Washington tandem Van de Graaff accelerator. The bombarding energies chosen easily satisfy the sub-Coulomb assumption. This was further checked for ^{12}C and ^{16}O projectiles with measurements at much higher energies. A detailed discussion of the experimental arrangement will be presented in a later publication.[12] Data were taken with symmetric detectors at $\theta_{lab}=\pm 30°$, $\pm 140°$, etc., and a 1-mm-wide strip ^{208}Pb target to virtually eliminate sensitivity to beam motion. At energies of 20 MeV and higher the ratio of the integrated peak to the integrated background under the peak

was generally greater than 2×10^3. The corrections to the data for multiple scattering only exceeded 0.05% at energies less than 20 MeV. At energies greater than 20 MeV, background subtraction and multiple scattering introduced systematic errors of less than 0.03% and 0.02%, respectively. Counting statistics was the dominant contributing factor to the experimental error for all beam energies and angles.

Statistically averaged experimental data for $^{16}O+^{208}Pb$ at $\theta_{lab}=150°$, normalized to the theoretical calculations, are shown in Fig. 2. Similar results were obtained with sixteen other excitation functions measured with other projectiles and at other scattering angles. For each excitation function there is, on average, one normalization constant which is a function of detector solid angles and scattering angles and was determined in the least-square fits described below.

The data were quantitatively compared with the theoretical calculations by fitting the data with use of a potential of the form

$$V_{tot}=V_{Coul}+V_{sc}-a_1V_{Coul}^2/2\mu+a_2V_{pol}+a_3V_{cex}, \quad (4)$$

where $-V_{Coul}^2/2\mu$ is the effective potential describing the relativistic effect and the a_i are theoretical parameters. Both the a_i and the normalization constants for the data were determined in these fits. With all of the a_i set equal to 1, the four sub-Coulomb effects assume their nominal magnitudes. The calculations at energies less than 20 MeV are dominated by the atomic screening; therefore we chose to fit the data only at energies greater than 20 MeV in order to minimize sensitivity of the fit to any errors in the screening calculation. The fit over this energy domain was found to be insensitive to a_2 (the vacuum polarization parameter), and therefore a_2 was set equal to 1 in the fits described in the following discussion. This insensitivity can be understood by examining Fig. 2 where it can be seen that the anticipated deviation from Rutherford scattering caused by vacuum polarization changes by only 0.05% for $E_{lab}>20$ MeV.

A simple contour plot of χ^2/ν as a function of a_1 and a_3 with $\nu=376$ is shown in the upper right-hand corner of Fig. 3. As a function of a_1 and a_3, χ^2/ν has a long minimum whose major axis is given parametrically by the line $1.1a_1+a_3=2.43$. This long χ^2/ν minimum has the consequence that the linear combination $1.1a_1+a_3$ can be determined with some accuracy while the relative magnitudes of a_1 and a_3 cannot be determined with any accuracy. The absolute minimum of the χ^2/ν function occurs at $a_1=2.4$ and $a_3=-0.2$ with $\chi^2/\nu=0.940$. Choosing the nominal values $a_i=1$, corresponding to the original parameter-free calculation, gives $\chi^2/\nu=0.956$, 2–3 error bars away from the χ^2 minimum. In comparison, for $a_1=a_3=0$ (i.e., no relativistic effect or nuclear polarizability) χ^2/ν assumes the value 1.25, far outside the realm of possibility. Other fits consistent with these have also been obtained by fitting on a contracted data set in which all data points with $E_{lab}<30$ MeV have been excluded. One consequently concludes from all these fits that a linear combination of the relativistic effect and nuclear polarizability close to that predicted from the parameter-free calculations is needed to fit the data.

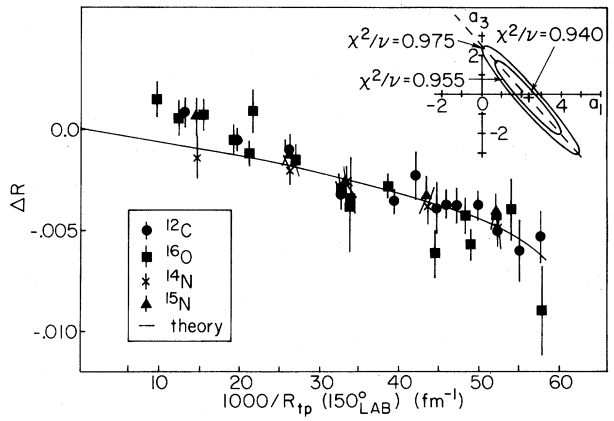

FIG. 3. Comparison of ΔR with the corresponding plot of the residual deviation from Rutherford scattering caused by nuclear polarizability and the relativistic effect. Inserted in the upper right-hand corner is a contour plot of χ^2/ν as a function of a_1 and a_3.

This residual deviation from Rutherford scattering caused by nuclear polarizability and the relativistic effect can be seen graphically in Fig. 3 where the quantity ΔR given by

$$\Delta R=R_{b/f}(\text{expt.})-R_{b/f}(\text{theory: screening+vacuum polarization}) \quad (5)$$

is plotted versus the inverse of the classical turning point $R_{tp}(150°(\text{lab}))$ for particles which scatter to $\theta_{lab}=150°$. The abscissa $(1000/R_{tp})$ is proportional to E_{lab} and allows one to superimpose data for all projectiles. The solid curve is the corresponding theoretically predicted ΔR for ^{16}O projectiles which

describes the relativistic effect and nuclear polarizability. (Similar calculations for ^{14}N, ^{15}N, and ^{12}C agree within 0.1% with this ^{16}O calculation.) In this figure the data for a given beam energy and projectile have been averaged over the measured backward scattering angles (θ_{lab} = 140°, 145°, 150°, etc.) in order to improve the statistics. It can be seen in Fig. 3 that above 20 fm^{-1} (which corresponds roughly to E_{lab} = 20 MeV for ^{16}O) the data agree substantially with the prediction, but below 20 fm^{-1} the data lie slightly above the prediction. This enhancement below 20 fm^{-1} may in part be caused by our neglect of atomic polarizability. It should be pointed out that the screening effect we are subtracting from the data to make this plot changes by more than 0.8% from 10 to 20 MeV; thus a 10% underestimation of this screening effect could give rise to the discrepancy.

In summary we have seen unambiguous evidence for the presence of a combination of nuclear polarizability and the relativistic effect. It is not possible from numerically fitting the data *alone* to determine the relative importance of these two effects. Nevertheless, if one sets nuclear polarizability at its normal value with a 25% error one has a measurement of relativistic dynamics with 30% accuracy. By taking the opposite tack and assuming the validity of relativistic dynamics, one has a measurement of averaged nuclear polarizability with 25% accuracy. Static electron screening appears to be reasonably accurate (to within 10%) while the measurement of vacuum polarization was masked by the uncertainties in atomic screening.

This work was supported in part by the U. S. Department of Energy.

[a]Present address: NSCL, Michigan State University, East Lansing, Mich. 48824.
[b]Present address: Nuclear Physics Laboratory, University of Colorado, Boulder, Colo. 80309.
[c]Present address: Westinghouse, Hanford, Wash.

[1]K. Alder and A. Winther, *Electromagnetic Excitation* (North-Holland, Amsterdam, 1975).
[2]J. Rasmussen *et al.*, Nucl. Phys. A341, 149 (1980).
[3]W. Schäfer *et al.*, Nucl. Phys. A272, 493 (1976).
[4]K. C. Wang *et al.*, Phys. Lett. 79B, 170 (1978).
[5]T. E. O. Ericson and J. Hüfner, Nucl. Phys. B47, 205 (1972).
[6]G. Baur *et al.*, Nucl. Phys. A288, 113 (1977).
[7]J. Ahrens *et al.*, Nucl. Phys. A251, 479 (1975).
[8]E. G. Fuller and Evans Hayward, in *Nuclear Reactions*, edited by P. M. Endt and P. B. Smith (North-Holland, Amsterdam, 1962), Vol. II, p. 113.
[9]E. A. Uehling, Phys. Rev. 48, 55 (1935).
[10]L. W. Fullerton and G. A. Rinker, Jr., Phys. Rev. A 13, 1283 (1976).
[11]C. W. Nestor, private communication; C. C. Lu *et al.*, At. Data 3, 1 (1971).
[12]W. G. Lynch *et al.*, to be published.

Measurement of the g Factor of the ^{237}Pu Short-Lived Fission Isomer

M. H. Rafailovich, E. Dafni,[a] G. Schatz,[b] S. Y. Zhu,[c] K. Dybdal,[d] S. Vajda, C. Alonso-Arias, and G. D. Sprouse
Department of Physics, State University of New York, Stony Brook, New York 11794
(Received 29 December 1981)

The perturbed-angular-distribution method has been used to measure the g factor of the τ=122(10)-nsec fission isomer in ^{237}Pu. To eliminate unwanted perturbations, a special cubic nonparamagnetic alloy, $^{235}UIr_2$, was heated to 950 °C and used as the target. The quantities measured were $A_{22}=+0.21(6)$ and $g=-0.45(3)$. The g factor is consistent with the $I=\frac{5}{2}$ ground state of the 871 $\frac{1}{2}^+$ Nilsson orbital, and the fission anisotropy is consistent with $K=\frac{1}{2}$ at the second saddle point.

PACS numbers: 21.10.Ky, 21.10.Pc, 27.90.+b

The fission isomers offer a unique opportunity to study nuclear structure at large deformations, and several beautiful experiments[1,2] have shown that the isomers have axis ratios of the order of 2 to 1. With the exception of ^{239}Pu,[3] more detailed information on the structure of these interesting nuclei has not yet been obtained because of the difficulty of making magnetic-moment measurements in the actinides. The perturbed-angular-distribution technique usually employed for g-factor measurements of isomeric states requires that the nuclear alignment be preserved